TÜBİTAK

Turkish Journal of Electrical Engineering & Computer Sciences

http://journals.tubitak.gov.tr/elektrik/

Research Article

Turk J Elec Eng & Comp Sci
(2016) 24: 3976 – 3986

doi:10.3906/elk-1502-162

Common spatial pattern-based feature extraction from the best time segment of BCI data

Önder AYDEMİR*
Department of Electrical and Electronics Engineering, Karadeniz Technical University, Trabzon, Turkey

Received: 18.02.2015 • **Accepted/Published Online:** 28.06.2015 • **Final Version:** 20.06.2016

Abstract: Feature extraction is one of the most crucial stages in the field of brain computer interface (BCI). Because of its ability to directly influence the performance of BCI systems, recent studies have generally investigated how to modify existing methods or develop novel techniques. One of the most successful and well-known methods in BCI applications is the common spatial pattern (CSP). In existing CSP-based methods, the spatial filters were extracted either by using the whole data trial or by dividing the trials into a number of overlapping/nonoverlapping time segments. In this paper, we developed a CSP-based moving window technique to obtain the most distinguishable CSP features and increase the classifier performance by finding the best time segment of electroencephalogram trials. The extracted features were tested by using support vector machines (SVMs). The performance of the classifier was measured in terms of classification accuracy and kappa coefficient (κ). The proposed method was successfully applied to the two-dimensional cursor movement imagery data sets, which were acquired from three healthy human subjects in two sessions on different days. The experiments proved that instead of using the whole data length of EEG trials, extracting CSP features from the best time segment provides higher classification accuracy and κ rates.

Key words: Common spatial pattern, moving window, cursor movement imagery, feature extraction, support vector machines

1. Introduction

Developments in the field of brain computer interface (BCI) research not only allow paralyzed people to use electronic devices, such as computers, neuroprostheses, and robotic arms [1], but also make other functions possible, including motor restoration, communication, environmental control, and even entertainment [2–4]. Electroencephalogram (EEG) is the most used signal acquisition method for BCI designs, mainly due to its fine temporal resolution, noninvasiveness, easy implementation, and low set-up costs [5]. In order to make BCI systems practical in use, researchers have attempted to improve the speed and accuracy of all components of BCI systems [6].

Current EEG-based brain computer interfaces are generally performed in five main components, which are signal acquisition, preprocessing, feature extraction, classification, and device control interface. Among these steps, feature extraction, which is necessary for representing input signals in a reduced feature space and for identifying discriminative information for different types of imagery EEG signals, has received the most attention from the BCI research community. Importantly, its capability directly influences the performance

*Correspondence: onderaydemir@ktu.edu.tr

of the BCI. However, it requires a lot of research to extract informative features among the existing feature extraction techniques or from a newly developed technique.

Various feature extraction techniques have been used in the BCI literature such as common spatial pattern (CSP) [7,8], Fourier transform [9], wavelet transform [10], power spectral density analysis [11], filtering methods [12,13], polynomial coefficients [6], and autoregressive model [14,15]. Amid these techniques, CSP is one of the very widely used feature extraction techniques in motor imagery-based BCI applications. In such CSP-based studies, researchers have designed different approaches to construct spatial filters whose variances contained the most discriminative information, and which also help to increase the classification accuracy (CA) of BCIs. Ramoser et al. applied their CSP-based method to the single-trial EEG, recorded from three subjects with 56 electrodes during left- and right-hand movement imagery. They investigated alternative optimal spatial filters design according to the importance of the electrodes [7]. In another CSP-based study, Kang et al. proposed two methods to obtain a composite spatial filter, which was a weighted sum of covariance matrices involving all five participating subjects. They used the BCI competition III dataset IVa, which was recorded with 118 electrodes during the imagination of the right hand and foot. Their results showed that it was useful for cases where pretrained CSP features need to be adapted to a subject with a low number of training samples [8]. In another approach, Novi et al. applied their method to the dataset IVa from BCI competition III, which recorded five subjects during the imagination of the left hand, right hand, and right foot movements. In order to achieve optimal spatial filters, they firstly decomposed the EEG signals into subbands and then extracted CSP features from those of subbands. Then they decided the most optimal subband(s) that provided more information for classifying the EEG trials [16]. In a time segmentation-based CSP study, Ghaheri and Ahmadyfard used dataset IIa from BCI competition IV, and instead of extracting CSP features from the whole data (one time segment), they divided the data into several time segments (the length of the time segments varied from 0.5 to 3 s with a step size of 0.5 s) and extracted CSP features from each time segment, separately. They used all the extracted features for classification [17]. Similarly, in another time segmentation-based CSP study, Asensio-Cubero et al. used dataset IIa from BCI competition IV. They made a comparison by applying CSP to three different segmentation types: 1) no segmentation, by applying CSP directly to the whole data trial, 2) uniform segmentation without overlapping, and 3) segmentation with overlapping [18]. [17] and [18] required a whole data trial to extract features at the test stage. Although many CSP-based methods have been reported that are relatively successful and accurate, they are not satisfactory in terms of speed and classification accuracy. In this work, instead of using the whole data length of EEG trials, we proposed a CSP-based moving window technique to obtain the most distinguishable CSP features by finding the best time segment of the electroencephalogram trials. Therefore, the main contribution of this time segmentation technique is that it provides the most informative segment of trial, increases classifier performance, and does not require a whole data trial at the test stage.

We applied the proposed algorithm to the EEG signals recorded from three healthy subjects during the motor imagery of two-dimensional cursor movements. The extracted features were tested with support vector machines (SVMs). We measured the effectiveness of the classifier in terms of CA and kappa coefficient (κ). With overall achieved CA and κ results, our method proves to have significant potential for designing alternative optimal spatial filters and classifying cursor movement imagery BCI signals.

2. Data set description

In this study, the Brain Quick EEG system (Micromed, Italy) was used to acquire EEG signals. The brain activity was sampled at 256 Hz and filtered between 0.1 and 120 Hz. Additionally, a 50-Hz notch filter was used to eliminate line noise. Eighteen EEG electrodes (Table 1) were located according to the international 10–20 system and were referenced to the electrode Cz. Because EOG and EMG artifacts were strong on the Fp1, Fp2, O1, and O2 electrodes, they were not selected for analysis [19,20]. The data acquisition equipment is given in Figure 1.

Table 1. List of electrodes.

Channel number	Channel name
1	Fp2
2	Fp1
3	F4
4	F3
5	F8
6	F7
7	Fz
8	T4
9	T3
10	C4
11	C3
12	T6
13	T5
14	P4
15	P3
16	Pz
17	O1
18	O2

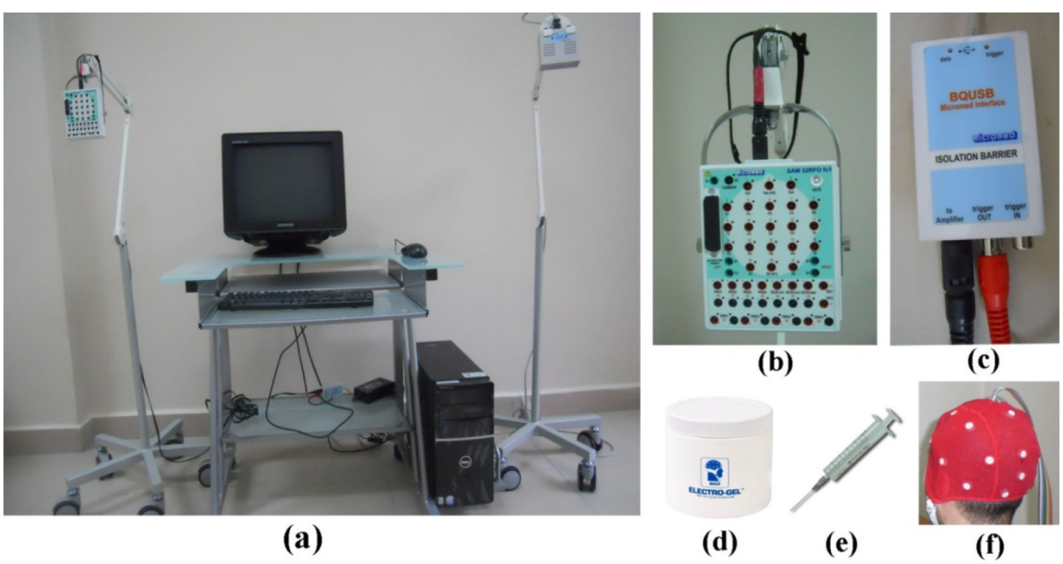

Figure 1. EEG data acquisition system: (a) full equipment, (b) amplifier, (c) isolation barrier, (d) electrode gel, (e) gel injection syringe, (f) electrode cap.

EEG signals were collected from three healthy male adults (subjects A, B, and C, aged 24, 24, and 29 years old, respectively) on two different offline sessions with a 1-week interval. The subjects who expressed willingness to participate in the experiment were well-rested, had normal blood pressure, and had slept more than seven hours the night before. Each trial began with a 2-s delay and then played a starting beep sound for 1 s. At 4 s, a target appeared in one of four possible positions (up, left, down, or right) on the middle edge, and after the target entered on the screen, a cursor appeared at its center and the subject had to perform a motor imagery task corresponding to the target for 8 s. Each trial ended with a beep sound. The timing scheme and stimulus interface are shown in Figure 2. It is worthwhile mentioning that this experimental protocol was approved by the Ethics Committee of Trabzon Clinical Researchers.

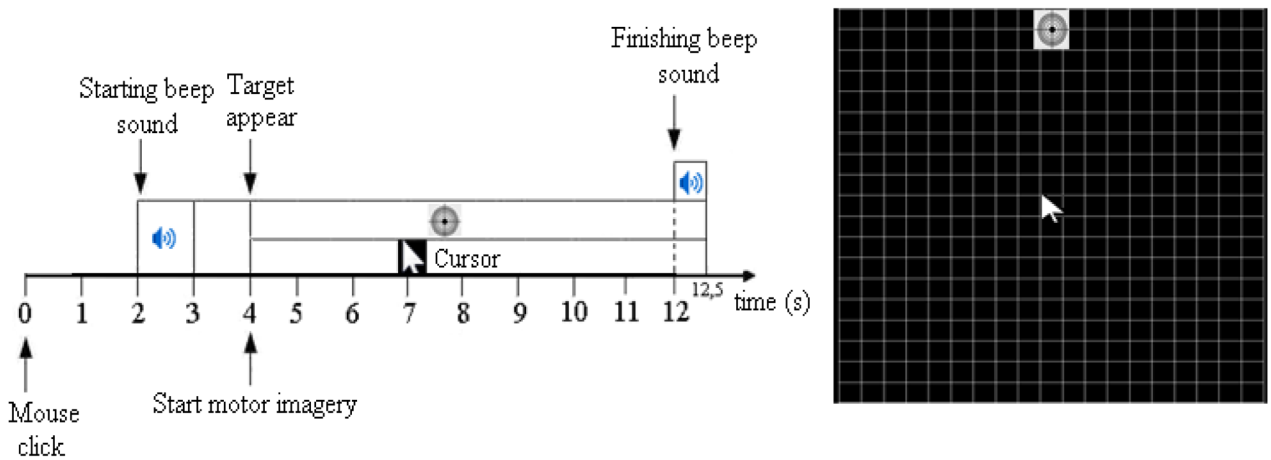

Figure 2. Timing scheme (left) and stimulus interface (right).

The first session trials were used as a training set, and the second session trials were used as the testing set. Table 2 shows the total number of considered trials for each subject. Both the training and testing sets consisted of an equal number of trials for each class.

Table 2. Total number of the considered trials.

Subject	Number of training set trials	Number of test set trials
A	140	152
B	148	152
C	148	152

The trial signals in both training and testing sets were assigned as follows: T1 = cursor up, T2 = cursor right, T3 = cursor down, and T4 = cursor left.

3. Methodology

3.1. Common spatial pattern

We extracted the features by applying CSP, which is one of the most popular and well-known feature extraction methods in motor imagery BCI studies [21,22]. The CSP method gives spatial filters, which maximize the variance of one class while minimizing the variance of the other class at the same time [7]. It is worthwhile to mention that to compute optimal CSP, all channels (except Fp1, Fp2, O1, and O2) were considered, and 10-fold cross validation (10-FCV) was used. The normalized spatial covariance matrix of an EEG trial is calculated as follows:

$$M = \frac{DD^T}{trace(DD^T)}, \tag{1}$$

where D denotes a trial that is CxS matrix (C is the number of channels and S is the number of samples). *trace* is the sum of the diagonal elements of (DD^T). The spatial covariance matrix was calculated by averaging over the trials of each class. Then two resultant matrices (one is for first class, the other is for second class) were summed and a composite covariance matrix M_C was obtained as

$$M_C = \bar{M}_1 + \bar{M}_2 \tag{2}$$

M_C can be factored into its eigenvectors as

$$M_C = E_C \lambda_C E_C^T, \tag{3}$$

where E_C is the matrix of eigenvectors and λ_C is the diagonal matrix of eigenvalues. Then a whitening transformation (W), which equalizes the variances in eigenspace, was calculated as follows:

$$W = \sqrt{\lambda_C^{-1}} E_C^T \tag{4}$$

W was used to transforms the average covariance matrices as

$$K_1 = W\bar{M}_1 W^T \text{ and } K_2 = W\bar{M}_2 W^T \tag{5}$$

Then K_1 and K_2 share common eigenvectors, and the sum of the corresponding eigenvalues for the two matrices is always equal to 1, such that

$$K_1 = U\lambda_1 U^T, \quad K_2 = U\lambda_2 U^T,$$

$$\lambda_1 + \lambda_2 = I, \tag{6}$$

where I is the identity matrix. Finally, a projection matrix $P = (U^T W)^T$, where the columns P^{-1} are the common spatial patterns and can be seen as time-invariant EEG source distribution vectors. With the projection matrix, the decomposition of a trial D was calculated as follows:

$$Z = PD \tag{7}$$

Since the sum of the corresponding eigenvalues is always one, the variances of the first and last rows of Z are suitable features for classification. In this study, we used the variances of the first and last rows as features. The variance was calculated as follows:

$$V = \frac{\sum \left(Z_R - \overline{Z_R}\right)^2}{L-1}, \tag{8}$$

where Z_R is a row of Z and L is the length of this row.

3.2. Classification algorithm and kappa coefficient

In this study, we tested the proposed algorithm with SVM. Due to the fact that it is a well-known classifier algorithm, we only gave its considered properties. We utilized the most commonly used radial basis function kernel. This kernel function was specified by the scaling factor σ. The most suitable σ value was searched in the interval between 0.1 and 2.0 (step size of 0.1). The 10-FCV technique was used to determine the best value of σ so as to maximize the classification performance. To implement the SVM algorithm, the *svmclassify* (with *svmtrain*) function of the MATLAB R2014a Bioinformatics Toolbox was used [10].

In order to evaluate the performance of the classifier, we calculated the CA and κ. CA was defined as the percentage of the number of trials classified correctly over the size of the data set, and κ was defined as the proportion of correctly classified samples after accounting for the probability of chance agreement [23]. It was calculated as follows:

$$Kappa = \frac{\Pr(A) - \Pr(E)}{1 - \Pr(E)}, \tag{9}$$

where *Pr(A)* represents the actual observed agreement and *Pr(E)* represents the probability of expected agreement by chance.

A κ value might range between 1 and -1, which corresponds to a perfect and a completely incorrect classification, respectively. On the other hand, a κ with value 0 indicates that the performance is equal to a random guess.

3.3. Feature extraction

Instead of using the whole data length (T = 8 s), in order to improve the classification accuracy rate, the best informative CSP-based features were sought in the whole EEG trials by a moving window. This window, which is illustrated with a bold frame in Figure 3, has two kinds of parameters: 1) a shifting parameter, which indicates how far the window is from the beginning point (T = 0 s), and 2) a length parameter, indicating the extension of the window, which has a start time (ST) and an end time (ET) point. ST is also equal to the shifting parameter, and ET $>$ ST.

In order to implement more experiments and approve their efficiency, the proposed method was performed on each combination of two-task pairs. In a two-task pair, the best window parameters are determined by the training set as follows:

Step 1: The algorithm starts at ST = 0 (no shifting) and ET = 0.2 s. Under these circumstances, the considered classifier is trained with the 10-FCV technique. This is called a window step (WS).

Step 2: For the next WSs, the ET parameter is set to a value between 0.4 and 8 with a step size of 0.2. In each WS, all 10-FCV classification accuracy results are stored with the considered WS parameters. The first two steps are called a loop. In each loop, the overlapped segmentation technique was used.

Step 3: For the next loop, the window is shifted by 0.2 s and the first two steps are repeated under the circumstance of ET $>$ ST.

Step 4: The algorithm is ended until ST and ET are set to 7.8 and 8, respectively. In total there are 40 loops and 820 WSs.

Step 5: Finally, the best window parameters, which provide the highest 10-FCV classification accuracy result, are determined among these 820 WSs. Figure 4 summarizes these five steps.

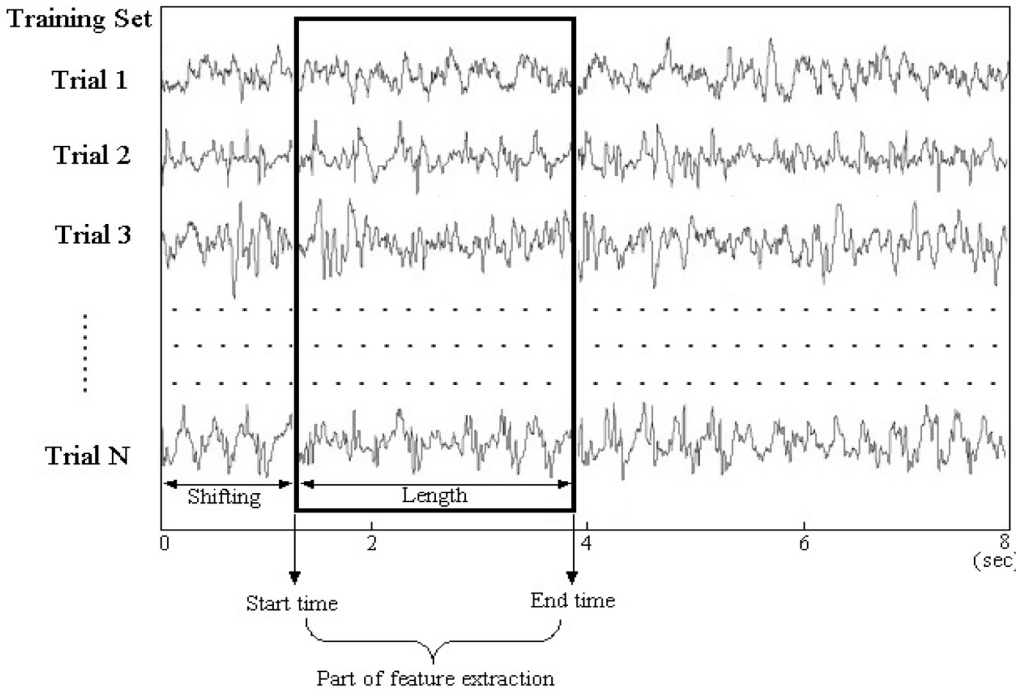

Figure 3. Seeking the best CSP features of the training set.

```
for ST= 0:0.2:7.8
    for ET=0.2:0.2:8
        if ET>ST
            RUN WINDOW STEP
        end
    end
end
```

Figure 4. Summary of the proposed algorithm.

4. Results

In the following subsections, the training, the test accuracy results of the classification algorithms, and the performance comparison are presented.

4.1. Training results

To obtain the best window and classifier parameters, 10-FCV technique was applied to each individual training data set. The cross-validation classification accuracy results and the best window parameters are presented in Table 3.

The best window parameters, ST and ET, are given under the results of cross-validation classification accuracy. As seen in the table, the optimum time segment might be selected from the beginning, the middle, or the last part of the trials. The cross-validation classification accuracies of Subject A fell in the range of 68.95% and 96.64%, whereas they were between 64.69% and 71.50% for Subject B, and between 68.89% and 73.77% for Subject C. On the other hand, the shortest and longest time segments were determined as 0.8 s and 6.8 s, respectively.

Table 3. Training accuracy results.

Task Pair	A	B	C
T1–T2	96.64 (ST = 0.2, ET = 1.2)	67.32 (ST = 0, ET = 6.0)	69.47 (ST = 2.2, ET = 4.8)
T1–T3	70.20 (ST = 2.8, ET = 7.0)	64.69 (ST = 0.6, ET = 6.0)	73.77 (ST = 5.4, ET = 6.4)
T1–T4	91.43 (ST = 0, ET = 1.8)	70.24 (ST = 0.4, ET = 4.6)	70.36 (ST = 1.2, ET = 8.0)
T2–T3	83.68 (ST = 0, ET = 1.0)	69.91 ST = 3.0, ET = 4.0)	68.89 (ST = 0, ET = 6.0)
T2–T4	68.95 (ST = 1.4, ET = 2.4)	70.48 (ST = 1.6, ET = 6.4)	71.30 (ST = 6.6, ET = 7.6)
T3–T4	69.40 (ST = 1.4, ET = 4.0)	71.50 (ST = 2.0, ET = 6.4)	70.75 (ST = 4.8, ET = 6.0)

4.2. Test results

Based on the obtained window and classifier parameters, the calculated CA and κ results for the SVM algorithm are given in Table 4. On the other hand, the CA and κ results, obtained by using the whole data length, are given in Table 5. It is worthwhile to mention that the same validation procedure was used in the training stage when the whole data length results were calculated. The average classification accuracy (ACA) and average κ (Aκ) results are also provided and given in the last two columns of these two tables. The achieved best CA and κ results for each task pair are written in bold font.

Table 4. Test accuracy results of the proposed method.

Task pair	A		B		C		Average	
	CA	κ	CA	κ	CA	K	CA	κ
T1–T2	**98.68**	**0.97**	65.79	0.32	67.11	0.34	77.19	0.54
T1–T3	**71.05**	**0.42**	65.79	0.32	**76.32**	**0.53**	**71.05**	**0.42**
T1–T4	93.42	0.87	**68.42**	**0.37**	71.05	0.42	**77.63**	**0.55**
T2–T3	**81.58**	**0.63**	65.79	0.32	68.42	0.37	71.93	0.44
T2–T4	64.47	0.29	**71.05**	**0.42**	**72.37**	**0.45**	69.30	0.39
T3–T4	68.42	0.37	**69.74**	**0.40**	**71.05**	**0.42**	**69.74**	**0.40**

As seen in Table 4, the highest CA and κ were achieved for the T1–T2 task pair of Subject A as 98.68% and 0.97, respectively. In this case, the determined best time segment parameters were ST = 0.2 s and ET = 1.2 s. On the other hand, the worst CA and κ were calculated for the T2–T4 task pair of Subject A as 64.47% and 0.29, respectively. In this case, the best time segment parameters were ST = 1.4 s and ET = 2.4 s. Nevertheless, according to the average values, the achieved highest CA and κ were also obtained for the T1–T4 task pair as 77.63% and 0.55, respectively. In contrast, the worst ACA and Aκ were obtained for the T2–T4 task pair with 69.30% and 0.39, respectively.

As can be seen in Table 5, the best CA and κ were obtained for the T1–T4 task pair of Subject A as 64.47% and 0.29, respectively. Additionally, the worst CA and κ performance were calculated for the T1–T3 task pair of Subject B as 48.68% and –0.03, respectively. Based on average values, while the best ACA and Aκ performances were achieved for the T1–T4 task pair as 61.40% and 0.23, respectively, the worst case was obtained for the T1–T3 task pair as an ACA of 52.63% and an Aκ of 0.05.

Table 5. Test accuracy results for the whole data length.

Task pair	A		B		C		Average	
	CA	K	CA	κ	CA	κ	CA	κ
T1–T2	57.89	0.16	50.00	0.00	56.58	0.13	54.82	0.10
T1–T3	52.63	0.05	48.68	–0.03	**56.58**	**0.13**	52.63	0.05
T1–T4	**64.47**	**0.29**	**60.53**	**0.21**	**59.21**	**0.18**	**61.40**	**0.23**
T2–T3	53.95	0.08	55.26	0.11	**55.26**	**0.11**	54.82	0.10
T2–T4	51.32	0.03	**59.21**	**0.18**	**60.53**	**0.21**	**57.02**	**0.14**
T3–T4	52.63	0.05	63.16	0.26	59.21	0.18	58.33	0.16

4.3. Performance comparison

In order to approve its effectiveness, we compare the performance of the proposed moving window method with the test CA results obtained by using the whole data length. A close observation of the results in Tables 4 and 5 reveals that the CA values of the proposed method are greater than those of the whole data length results for all subjects and task pairs. Although the best CA performance of the proposed method was achieved as 98.68% for the T1–T2 task pair of Subject A, for the same task pair the highest CA was only obtained as 57.89% for the whole data length. In contrast, while the best CA performance of the whole data length was obtained as 64.47% for the T1–T4 task pair of Subject A, in the same case, the proposed method yielded better performance as 93.42% CA. Based on the values of ACA, whereas the highest ACA of the proposed method was calculated as 77.63% for the T1–T4 task pair, the highest ACA was calculated as 61.40% by using the whole data length for the same task pair.

The results of the proposed method also outperformed the whole data length results in terms of κ. Similar to the CA results, whereas the best κ performance of the proposed method was obtained as 0.97 for the T1–T2 task pair of Subject A, for the same task pair the highest κ was obtained only as 0.16 for the whole data length. On the other hand, while the best κ performance of the whole data length was calculated as 0.29 for the T1–T4 task pair of Subject A, the proposed method achieved a better κ performance of 0.87 for the same task pair.

5. Discussion and conclusion

In this paper we proposed a moving window technique for increasing the classification accuracy and κ rates of cursor movement imagery EEG signals by selecting the best time segment of the EEG trials. Our approach was successfully applied to the 6 different task pairs of each three subjects. Experiments proved that instead of using whole data length, extracting CSP features from the best time segment of EEG trials provides higher CA and κ rates for all 18 task pairs (6 task pairs from each three subjects). The proposed moving window technique improved the ACA and Aκ rates for all binary task pairs.

It is worthwhile to mention that it was crucial to prove the robustness and applicability of the proposed method due to the fact that it provided discriminative features both in the training and in the testing sets, which were collected during two different sessions with about a 1-week interval.

Another positive attribute of the proposed method was that it was not necessary to use the whole length of the EEG trials, which, importantly, helped to reduce the computational time of the test trials. For example, for the T1–T2, T2–T3, and T2–T4 task pairs of Subject A, the length of the best time segment was only 1 s. Moreover, the length of the longest time segment, which was obtained for the T1–T4 task pair of Subject C, was also 1.2 s shorter than the whole data length.

In our previous study [10], the most suitable time segment was determined by the ET parameter, which provided the highest classification accuracy, whereas the ST parameter was kept constant at 0. However, the best obtained window parameters (ST and ET) in this study showed that instead of keeping the ST parameter constant at 0, using the proposed moving window technique provided the most appropriate time segment.

The main disadvantage of the proposed method was its time-consuming length in the training section. However, it is worth mentioning that it provided a fast and accurate EEG-based BCI system at the testing stage.

Based on these results, we think that the proposed moving window-based method has great alternative potential to extract informative CSP features in increasing the classification accuracy and κ rates and reducing the testing time in designing BCI applications.

Acknowledgment

The author would like to thank all the subjects who were associated with the acquisition of the data set.

References

[1] McFarland DJ, Sarnacki WA, Wolpaw JR. Electroencephalographic (EEG) control of three-dimensional movement. J Neural Eng 2010; 7: 1-21.

[2] Daly JJ, Wolpaw JR. Brain–computer interfaces in neurological rehabilitation. Lancet Neurol 2008; 7: 1032-1043.

[3] Gao X, Xu D, Cheng M, Gao S. A BCI-based environmental controller for the motion-disabled. IEEE T Neur Syst Reh 2003; 11: 137-140.

[4] Zhao Q, Zhang L, Cichocki A. EEG-based asynchronous BCI control of a car in 3D virtual reality environments. Chinese Sci Bull 2009; 54: 78-87.

[5] Menon C, de Negueruela C, Millán JDR, Tonet O, Carpi F, Broschart M, De Rossi D. Prospects of brain–machine interfaces for space system control. Acta Astronaut 2009; 64: 448-456.

[6] Kayikcioglu T, Aydemir O. A polynomial fitting and k-NN based approach for improving classification of motor imagery BCI data. Pattern Recogn Lett 2010; 31: 1207-1215.

[7] Ramoser H, Muller-Gerking J, Pfurtscheller G. Optimal spatial filtering of single trial EEG during imagined hand movement. IEEE T Rehabil Eng 2000; 8: 441-446.

[8] Kang H, Nam Y, Choi S. Composite common spatial pattern for subject-to-subject transfer. IEEE Signal Proc Lett 2009; 16: 683-686.

[9] Wang Y, Veluvolu KC, Lee M. Time-frequency analysis of band-limited EEG with BMFLC and Kalman filter for BCI applications. J Neuroeng Rehabil 2013; 10: 109-125.

[10] Aydemir O, Kayikcioglu T. Decision tree structure based classification of EEG signals recorded during two dimensional cursor movement imagery. J Neurosci Meth 2014; 229: 68-75.

[11] Trejo LJ, Rosipal R, Matthews B. Brain-computer interfaces for 1-D and 2-D cursor control: designs using volitional control of the EEG spectrum or steady-state visual evoked potentials. IEEE T Neur Sys Reh 2006; 14: 225-229.

[12] Li Y, Long J, Yu T, Yu Z, Wang C, Zhang H, Guan C. An EEG-based BCI system for 2-D cursor control by combining Mu/Beta rhythm and P300 potential. IEEE T Biomed Eng 2010; 57: 2495-2505.

[13] McFarland DJ, Miner LA, Vaughan TM, Wolpaw JR. Mu and beta rhythm topographies during motor imagery and actual movements. Brain Topogr 2000; 12: 177-186.

[14] Huan NJ, Palaniappan R. Neural network classification of autoregressive features from electroencephalogram signals for brain–computer interface design. J Neural Eng 2004; 1: 142-150.

[15] García-Laencina PJ, Rodríguez-Bermudez G, Roca-Dorda J. Exploring dimensionality reduction of EEG features in motor imagery task classification. Expert Syst Appl 2014; 41: 5285-5295.

[16] Novi Q, Guan C, Dat TH, Xue P. Sub-band common spatial pattern (SBCSP) for brain-computer interface. In: IEEE/EMBS 2007 Conference on Neural Engineering; 2–5 May 2007; Kohala Coast, HI, USA. New York, NY, USA: IEEE. pp. 204-207.

[17] Ghaheri H, Ahmadyfard AR. Extracting common spatial patterns from EEG time segments for classifying motor imagery classes in a Brain Computer Interface (BCI). Sci Iran 2013; 20: 2061-2072.

[18] Asensio-Cubero J, Palaniappan R, Gan J. A study on temporal segmentation strategies for extracting common spatial patterns for brain computer interfacing. In: IEEE 2011 UK Workshop on Computational Intelligence; 7–9 September 2011; Manchester, UK. New York, NY, USA: IEEE. pp. 99-102.

[19] Halder S, Bensch M, Mellinger J, Bogdan M, Kübler A, Birbaumer N, Rosenstiel W. Online artifact removal for brain-computer interfaces using support vector machines and blind source separation. Comput Intel Neurosci 2007; Article ID 82069.

[20] Zeng H, Song A. Removal of EOG artifacts from EEG recordings using stationary subspace analysis. Sci World J 2014; Article ID 259121.

[21] Lee KY, Kim S. Designing discriminative spatial filter vectors in motor imagery brain-computer interface. Int J Imag Syst Tech 2013; 23: 147-151.

[22] Grosse-Wentrup M, Buss M. Multiclass common spatial patterns and information theoretic feature extraction. IEEE T Biomed Eng 2008; 55: 1991-2000.

[23] Aydemir O, Kayikcioglu T. Wavelet transform based classification of invasive brain computer interface data. Radioengineering 2011; 20: 31-38.